International Journal of Fluid Power 10 (2009) No. 3 pp. 51-59

NUMERICAL AND EXPERIMENTAL INVESTIGATION ON O-RING-SEALS IN DYNAMIC APPLICATIONS

Alexander Wohlers[1], Oliver Heipl[1], Bo N. J. Persson[2], Michele Scaraggi[3] and Hubertus Murrenhoff[1]

[1]*Institute for Fluid Power Drives and Controls (IFAS), RWTH Aachen University, Steinbachstraße 53, 52074 Aachen, Germany*
[2]*Institut für Festkörperforschung (IFF), Forschungszentrum Jülich, 52425 Jülich, Germany*
[3]*DIMeG-Politecnico di Bari, V.le Japigia 182, I-70126 Bari, Italy*
alexander.wohlers@ifas.rwth-aachen.de, oliver.heipl@ifas.rwth-aachen.de, hubertus.murrenhoff@ifas.rwth-aachen.de, b.persson@fz-juelich.de, m.scaraggi@poliba.it

Abstract

This paper presents a physically-based simulation approach to predict the friction force at oil lubricated contacts for rubber o-ring seals in dynamic applications. In the boundary lubrication regime the friction coefficient is calculated using a recently developed contact mechanics theory. The stress and strain fields in the rubber are calculated using the finite element analysis (FEA). In the FEA the temperature-dependent nonlinear rubber behaviour is considered. Loads due to the assembly process, thermal expansion, system pressure and tangential friction forces are included in the analysis. In the mixed and hydrodynamic lubrication regimes, the asperity-asperity and fluid-asperity interactions are determined from the Persson's dry-contact mechanics theory, the Reynolds-equation (gap flow) and the deformation model of the seal. To test the theory a test rig has been developed. Simulation results, carried out for an unpressurized o-ring seal system, are compared to the experimental data and, especially for small velocities where mixed lubrication prevails, the results are in good agreement.

Keywords: hydraulics, pneumatics, o-ring seal, finite element analysis FEA, gap flow, rubber friction, contact mechanics, fluid structure interaction

1 Introduction

Seals play a crucial role in many modern engineering devices and the failure of seals may result in catastrophic events, such as the Challenger disaster. In many cases simple and inexpensive elastomeric seals such as o-rings, x-rings or rectangular rings, are used. However, the failures of seals usually result in expensive and time-consuming replacement procedures.

Nowadays the design process of seals and seal systems is mostly based on experimental investigations, which are complex and time consuming because of the wide range of variables involved in the seal operation.

Computationally aided methods are used in a wide range of engineering applications with the benefit of reducing development time and cost. The numerical treatment of hydraulic and pneumatic system behaviour is well established but, in the sealing technology, mainly static sealing calculations for smooth-surfaces have been performed.

In this paper a model for dynamic sealing systems is presented with the focus on the hydraulic piston o-ring seal system, see Fig. 1, for which the interfacial friction is calculated from the boundary lubrication regime to the hydrodynamic lubrication regime.

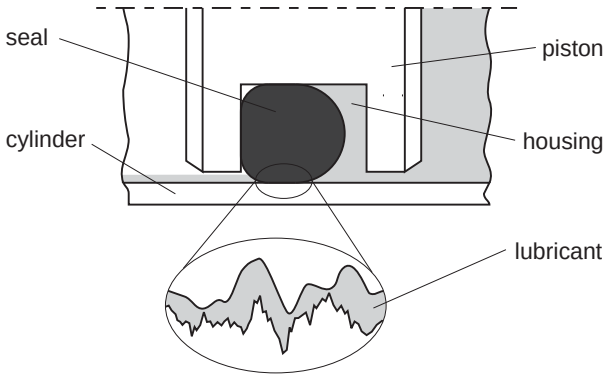

Fig. 1: *Hydraulic rubber o-ring seal system*

In Section 2, a brief review of the state of art on sealing research is presented. Section 3 describes the adopted numerical approach for static and dynamic sealing modelling. Section 4 describes the adopted experimen-

This manuscript was received on 8 July 2009 and was accepted after revision for publication on 9 October 2009

tal setup for testing the theory, while Section 5 presents a comparison between the predicted and the measured friction at the seal-cylinder interface. For small velocities, where mixed lubrication prevails, the results are in good agreement.

2 Current State of Research

The methods used in developing sealing systems are mostly based on research results from the middle of the last century. The challenge to describe an elastomeric seal regarding friction force and leakage was recognized by a few researchers about 60 years ago. Nevertheless, still no universally accepted model to describe the dynamical properties of seals exists.

The first serious investigation on elastomeric seals dates back to White and Denny (1947). Using a rectangular seal profile, they studied (experimentally) the transition from boundary to full hydrodynamic lubrication. Using the Reynolds equation, a simple numerical model was developed to predict the film thickness and hydrodynamic friction. An extension of this theory was described by Field and Nau (1975). The authors coupled the Reynolds equation with an elastic equation to study the elastohydrodynamic regime, with the measured contact stress distributions used as input. The great challenge of elastohydrodynamic simulation for soft materials such as elastomers was pointed out. A small change in pressure leads to a large deformation and the calculation tends to be unstable as long as no counteractive measure, e.g. under relaxation, were applied. Ruskell (1980) avoided these numerical problems by using a single equation containing the coupling between the hydrodynamic and the elastic behaviour. The contact pressure was conveyed by the FEA. Furthermore, a rapidly converging Newton-Raphson method was adapted. Increasing computer performances allowed Nikas (2003) the development of a new elastohydrodynamic model. In contrast to earlier publications, the contact pressure distribution was calculated by using structural mechanics equations based on the classic Hookian and the Mooney-Rivlin law. Öngün, André, Bartel and Deters (2008) studied the fluid dynamics (steady-state Reynolds equation) of a rubber o-ring. Using a commercial FEA package an approximately asymptotic relationship between contact pressure and separation were accomplished. Gropp and Freitag (2002) performed a finite element analysis to predict the contact pressure for more complex geometries. In the calculation of the hydrodynamic pressure build up they used a cavitation model.

The studies presented above assumed a full hydrodynamic lubrication. For mixed lubrication more involved models are necessary. Kanters (1991) investigated the influence of surface roughness on seal friction. To predict the static contact pressure a commercial FEA package was used. The flow factor approach was established by Patir and Cheng (1978 and 1979). A recently developed extension was presented by Salant, Maser and Yang (2007). They supplemented the roughness effect by implementing the contact mechanics model of Greenwood and Williamson (1966).

In the mixed and boundary lubrication regimes microscopic seal deformations arises in contact regions by touching asperities. A result of these periodical deformations is energy dissipation. Achenbach and Frank (2001) developed a model to describe elastomeric friction. Beside the hysteretic energy loss, an intermolecular bonding effect was described. For lip seals Wassink, Lenss, Levitt and Ludema (2001) additionally accounted for the energy loss in the fluid film. Recently, an investigation on the transition from boundary lubrication to full hydrodynamic lubrication for soft and elastic contact was performed by Persson and Scaraggi (2009).

Many efforts have been done within the last half a century to be able to describe seal systems. However detailed calculations of the friction force at the seal were not done. A reason for that could be the lack of theoretical models for rubber friction. Using a proven contact model and a physically-based rubber friction theory (Persson, 2001) in this paper the hysteretic deformation is calculated.

3 Numerical Modelling

A numerical model was developed in order to calculate the rubber friction at o-ring seals. The structure of the proposed model allows an extension of the simulation to more complex geometries in further steps. The general computational procedure is shown in Fig. 2.

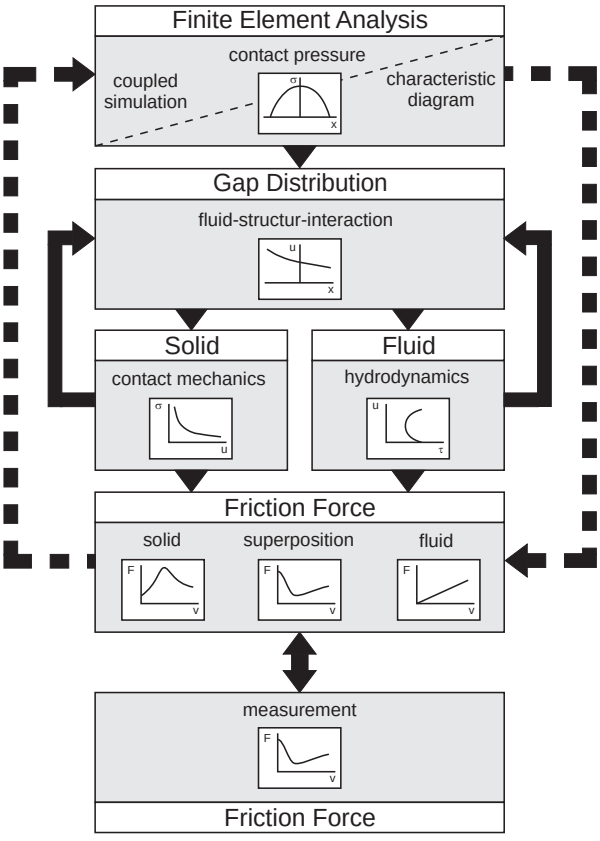

Fig. 2: *Structure of the elastohydrodynamic simulation model for hydraulic seal*

Beginning with a FEA using a commercial software package to determine the steady-state behaviour of the

elastomeric seal, a customised dynamic simulation follows. The contact pressure profile as well as the deformed shape of the seal are used as input for the consecutive dynamic simulation involving hydrodynamics and seal deformation. The shear stresses in the contact influence the seal shape and is included in the simulation (solid arrows in Fig. 2). Due to the friction force in the contact area the seal is elongated. The dashed arrows identify the coupling between the friction force and the FEA. Instead of a full online coupling an offline coupling using a characteristic diagram can be used. The FEA can also be used to calculate characteristic diagrams of the conditions in the gap for the non-moving case, which are shown in Section 3.1. These diagrams can be used in the design process of rubber o-ring seals.

3.1 Steady-State Simulation

In order to perform the analysis of the steady-state seal behaviour the FEA is used. The investigated system is modelled as axial-symmetric along the rod axis. The cross-section of the o-ring has a circular shape, groove and tube are build up from ideally flat geometries. The surfaces roughness is not being considered in the FEA but is included in a mean-field way in the dynamical model of Persson (see below). The nonlinear rubber properties are described using the Mooney-Rivlin constitutive model. For the unpressurized case where the strain is very small the two parameter of the model can be estimated in good approximation using the experimentally determined relationship to the temperature dependent hardness. In Fig. 3 the measured bulk modulus (real and imaginary part) is shown. The measurement was carried out with a strain amplitude of 0.5 % at a constant temperature of 17 °C. In the FEA the (real) elastic modulus for very small frequencies is used, while the constitutive relationship at higher frequencies is an important input for the rubber friction theory presented in Section 3.2.

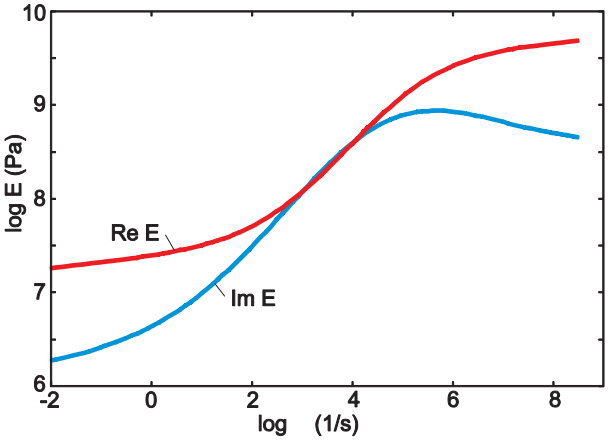

Fig. 3: *The measured real and imaginary part of the rubber viscoelastic modulus as a function of frequency for the strain amplitude 0.5 % and the temperature 17 °C*

The structural mechanics model enables the application of different types of load to the o-ring. An initial load is determined by geometrical parameters. The use of an axial-symmetric model enables also the calculation of the stresses due to the circular expansion of the seal. Different temperatures can be pre-set in the model. The thermal strain depends on the coefficient of thermal expansion of the rubber. Another possible load is a one-sided system pressure (in-chamber pressure) which is clearly only applied to not-contacting surface elements.

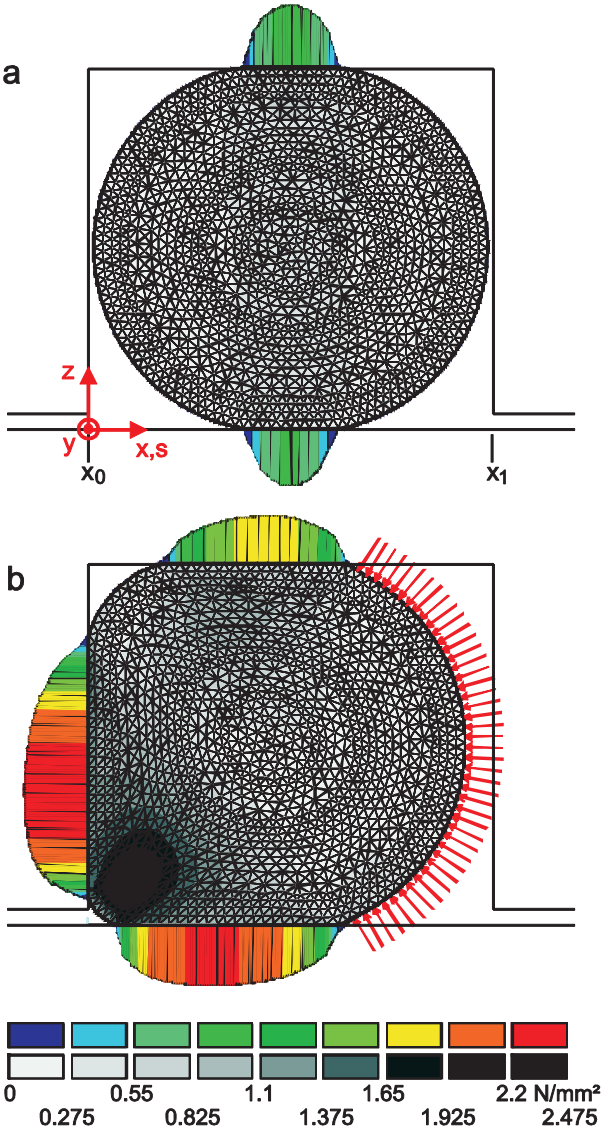

Fig. 4: *Contact pressure distribution and von Mises stresses of an O-Ring-Seal a) under initial compression at 20 °C and b) at 95 °C, with a system pressure of 10 bar and a specific friction force of 2.5 N per mm circumference*

Furthermore, in the contact region to the cylinder tube a friction force can be applied. This leads to an additional elongation of the seal. A combination of these different loads is shown in Fig. 4.

The FEA calculations can be used to obtain characteristic diagrams, such as the dependence of the contact pressure on the axial seal position. In Fig. 5 a few such diagrams are shown. The temperature is varied inside the application limits for the rubber material given by the seal manufacturer. The system pressure is varied between zero and 16 bar. The influence of temperature and pressure on the contact width, the maximum contact pressure and the contact force are depicted in Fig. 5.

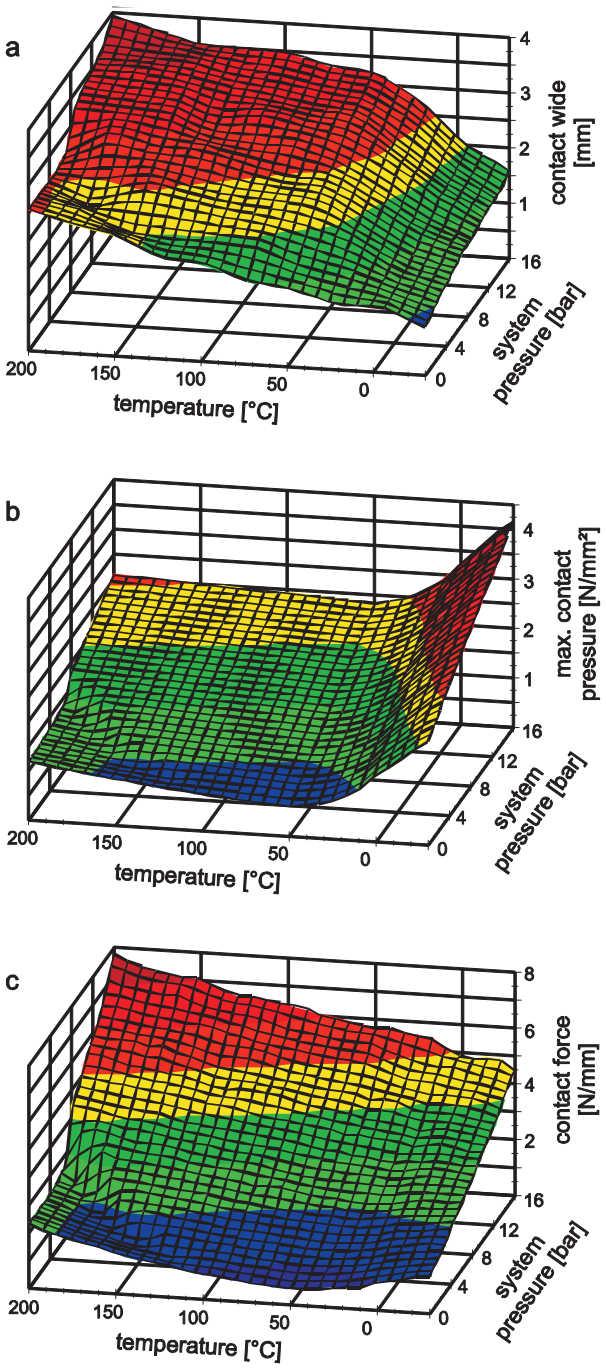

Fig. 5: *Characteristic diagrams from FEA, showing a) contact width, b) maximum contact pressure and c) contact force, as a function of the system pressure and the temperature*

3.2 From Boundary to (Soft-Elasto) Hydrodynamic Lubrication

Elastohydrodynamic simulations so far have been performed using two different approaches. Using an inverse method, the gap height can be computed by equalising hydrodynamic pressure and static contact pressure (Blok, 1963). This approach, which assumes full hydrodynamic lubrication, is limited in complexity and cannot be extended to general conditions. The second approach used below, is based on a direct method where the hydrodynamic pressure and the interfacial separation are obtained in an iterative way.

In general the local separation u between the seal surface and the cylinder tube can be calculated by combining the initial seal shape $u_0(x)$ with the elastic seal deformation $u_z(x)$. The initial seal shape can be calculated in the contact region by combining the FEA results of the contact pressure with Eq. 7. This allows considering the nonlinear deformation properties of the rubber.

$$u(x) = \bar{u}_z(x) + u_0(x) \tag{1}$$

The calculation of the elastic seal deformation due to hydrodynamic effects, which is by the way normally in the range of some µm, is based on Eq. 2 with the assumption of a linearly elastic material with a half plane response (Johnson, 2003).

$$\bar{u}_{z,p}(x) = -\frac{2\left(1-\nu^2\right)}{\pi E}\int_{x_0}^{x_1}\Delta p(s)\ln\left|x-s\right|ds\,. \tag{2}$$

In addition to this equation Johnson (2003) adds an extension to this equation to consider the influence of the axial distortion on the radial deformation,

$$\bar{u}_{z,q}(x) = \frac{(1-2\nu)(1+\nu)}{2E}\left(\int_{x_0}^{x}\tau(s)\,ds - \int_{x}^{x_1}\tau(s)\,ds\right). \tag{3}$$

Thereby a seal elongation caused by friction is realisable. However, in the present study we do not include the effect, as the seal material is incompressible (rubber).

As the hydrodynamic pressure not only results in a deformation but also in a lift-off, a comparison between static and dynamic forces has to be done. Therefore Eq. 4 provides an equilibration condition which influences the calculation of the seal deformation $u_z(x)$

$$\begin{aligned}&\int_{x_0}^{x_1}\left(p_{\text{cont,stat}}(s)+p_{\text{fluid,stat}}(s)\right)ds\\ &=\int_{x_0}^{x_1}\left(p_{\text{cont,dyn}}(s)+p_{\text{fluid,dyn}}(s)\right)ds\end{aligned} \tag{4}$$

The contact pressure $p_{\text{cont,stat}}$ results from the FEA calculation. In the dynamic simulation the contact pressure $p_{\text{cont,dyn}}$ is calculated using Eq. 7. The pressure drop from system pressure to ambient pressure over the static sealing gap (zero velocity) $p_{\text{fluid,stat}}$ as well as the hydrodynamic pressure $p_{\text{fluid,dyn}}$ for the dynamic case are calculated using the Reynolds-equation Eq. 6.

The local pressure differences $\Delta p(x)$ that leads to the deformation of the seal in Eq. 2 can be defined as the difference between dynamic and static local pressures

$$\Delta p(x) = p_{\text{fluid,dyn}}(x) + p_{\text{cont,dyn}}(x) - p_{\text{cont,stat}}(x) - p_{\text{fluid,stat}}(x) \tag{5}$$

The fluid pressure can be calculated using the Reynolds equation, which is in the general one-dimensional form

$$\frac{\partial}{\partial x}\left(\frac{u^3}{\eta}\frac{\partial p_{\text{fluid}}}{\partial x}\right) = 6U\left(\frac{\partial u}{\partial x}\right) + 12\frac{\partial u}{\partial t}\,. \tag{6}$$

For the case of non transient analysis, as done in this work, the squeeze film term in Eq. 6 becomes zero.

From Persson's contact mechanics theory the asymptotic (experimentally verified) exponential relation

between the squeezing pressure and the (average) separation can be derived:

$$p_{\text{cont}}(u) = \beta E^* \exp\left(-\alpha \frac{u}{h_{\text{rms}}}\right). \quad (7)$$

Figure 6 shows the cylinder surface topography as measured using an atomic force microscope (AFM). The surface shows an anisotropic texture caused by the manufacturing process.

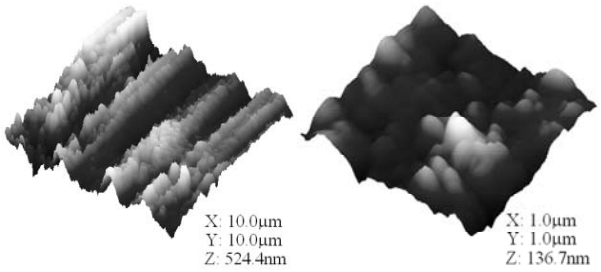

Fig. 6: *Surface topography at two different resolutions measured with an AFM*

The angular averaged power spectral density based on the AFM measurement data (2D-data) is shown in Fig. 7. To extend the measurement range a stylus instrument is used (1D-data).

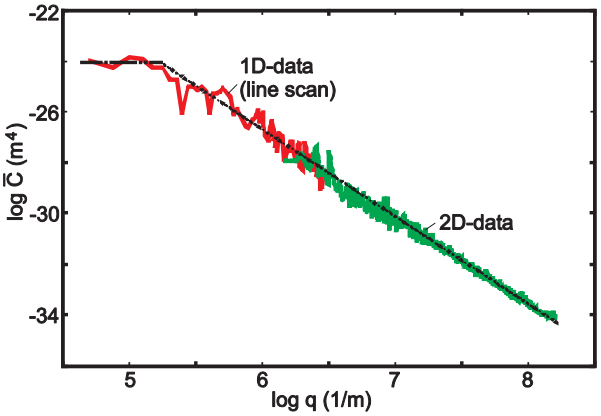

Fig. 7: *Angular averaged power spectral density for the polished steel surface shown in Fig. 6*

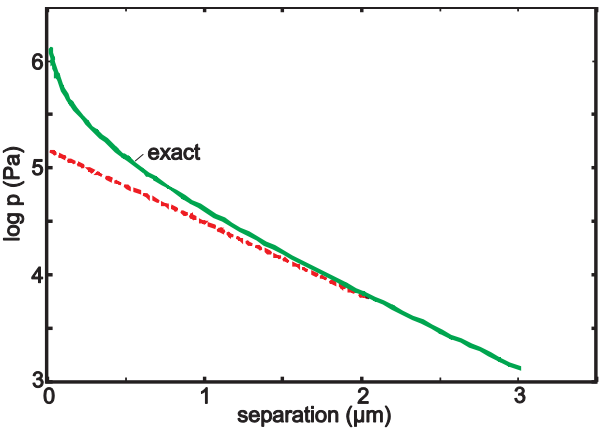

Fig. 8: *The exact calculation of the contact pressure as a function of the separation (solid line) and the asymptotic approximation (dashed line, Eq. 7)*

Figure 8 shows the exact calculation of the contact pressure (solid line) based on Persson's theory (2007) and the asymptotic result (dashed line, Eq. 7) as a function of the interfacial separation. Because of the small pressures which prevail in most seal systems it is legitimate to use the approximation given in Eq. 7.

The introduced equations have to be fulfilled at each node in the discrete calculation mesh. The solution algorithm has been extensively described in Persson and Scaraggi (2009).

The total friction force can be calculated by super positioning of friction force due to shear stresses in the fluid F_{fluid} and friction force due to shear stresses in the contact F_{cont}.

$$F_{\text{fric}} = F_{\text{cont}} + F_{\text{fluid}} \quad (8)$$

The viscous part of the friction is computed by integration of the local shear stresses over contact width and circumference

$$F_{\text{fluid}} = \pi d \int_{x_0}^{x_1} \tau(x)\, dx\,. \quad (9)$$

The fluid shear stresses can be derived from the (converged) hydrodynamic pressure profile

$$\tau = \eta \frac{U}{u} \pm \frac{u}{2} \frac{\partial p_{\text{fluid}}}{\partial x}\,. \quad (10)$$

The viscosity is usually measured at specific reference conditions p_0 and T_0. In general the dependency of the viscosity on the pressure and the temperature can be approximated using the approximation function

$$\eta(x) = \eta_0\, e^{\alpha_\eta (p(x)-p_0)}\, e^{-\beta_\eta (T(x)-T_0)}, \quad (11)$$

where α_η and β_η are coefficients that can be derived from viscosity measurements at different conditions. While the influence of a change in temperature is very high, the influence of the pressure dependency is negligible small for low system pressures.

The boundary friction is calculated by areal integration of the contact pressure profile,

$$F_{\text{cont}} = \pi d \int_{x_0}^{x_1} \mu\, p_{\text{cont}}(x)\, dx\,. \quad (12)$$

The coefficient of friction is calculated using the theory of Persson (2001) ,

$$\mu = \frac{1}{2} \int U \cdot \mathbf{q} C(\mathbf{q}) P(\mathbf{q}) \cdot \text{Im} \frac{E(\mathbf{q} \cdot U)}{(1-\nu^2)\sigma_0} dq_x dq_y \quad (13)$$

Figure 9 shows the calculated friction coefficient for the surface that is used within this work. This calculation is done with and without consideration of the flash temperature. The friction coefficient arises from the pulsating visco-elastic deformations of the rubber induced by the asperities on the hard counter surface.

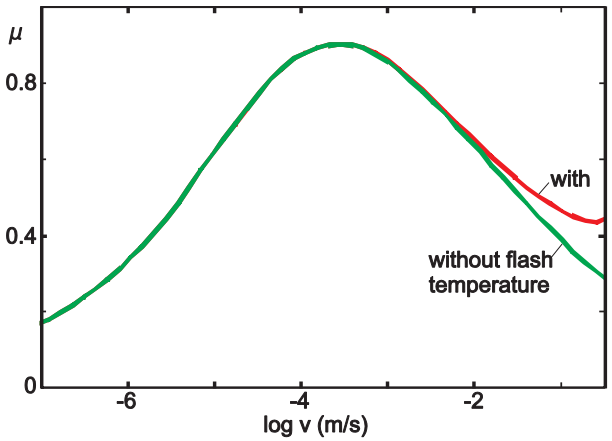

Fig. 9: *Calculated friction coefficient with and without consideration of the flash temperature using the Persson's theory*

4 Experimental Investigation

In order to obtain the friction at pneumatic and hydraulic sealing systems, a test rig is build-up. To measure the Stribeck-curve over a broad range also the high translational velocities, where pure hydrodynamic lubrication is present, is in the focus of the experimental studies. To achieve velocities up to 10 m/s, a cylinder tube test rig with high dynamic force compensation was developed, see Fig. 10. The cylinder tube is mounted inside the piston rod housing, and is driven by a crank mechanism. Due to the high resulting inertia forces (up to 30 kN at 2000 rpm) a mass force compensation gear box is designed.

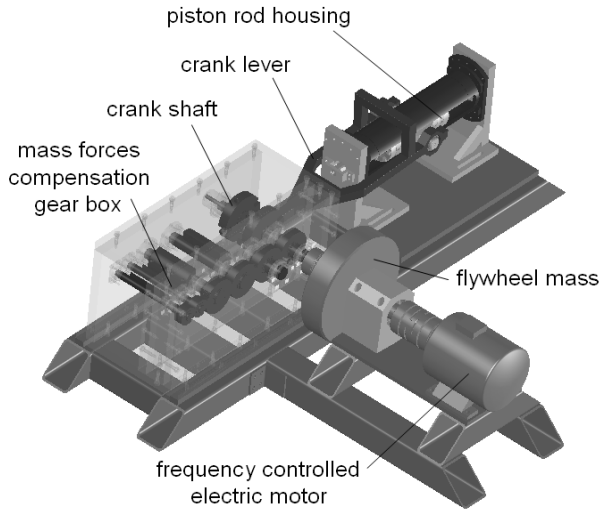

Fig. 10: *High velocity friction force test rig for pneumatic seals*

Figure 11 shows the measurement principle. The cylinder tube is in motion while the friction force at the test seal which is placed at the fixed test piston is measured using a piezoelectric force sensor. This principle allows measuring the friction at the test seal separately without having an influence of other frictional forces that occur. To apply a pressure at one side of the seal a second piston is used. The advantage of this concept is the non-varying pressurized capacity that guarantees a constant system pressure.

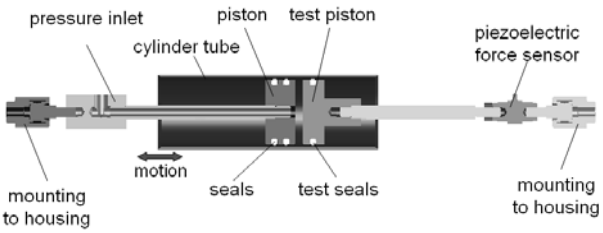

Fig. 11: *Friction force measurement principle*

5 Comparison of Measurement and Simulation

In order to validate the simulation model, friction force measurements are carried out with the parameters given in Table. 1. To simplify the problem the oil is not pressurized. In order to be able to compare measurement and numerical results, much attention should be paid to provide enough oil at the seal and therefore to avoid insufficient lubrication. However, due to the actual design, especially at high velocities, the case of starved lubrication can occur.

Table 1: Parameters of the investigated seal system

O-Ring	
Material	FKM 70
Cross-section diameter	6 mm
Inside diameter	52.63 mm
Groove	
Diameter of the ground	53.78 mm
Groove wide	6.3 mm
Cylinder tube	
Diameter	65 mm
RMS-Roughness	0.1 µm
Intermediary fluid	
Type	Fuchs Plantohyd 32 S
Viscosity at 25°C	47 mPas

Parallel to the measurements, calculations with the introduced model was performed. For reasons of computation time the full self-consistent solution to the FEA calculation of the macroscopic deformation of the rubber o-ring, and the calculation of the frictional shear stresses, was not performed. Figure 12 shows the simulated contact pressure profile, the fluid pressure profile, and the deformed seal shape for three different velocities.

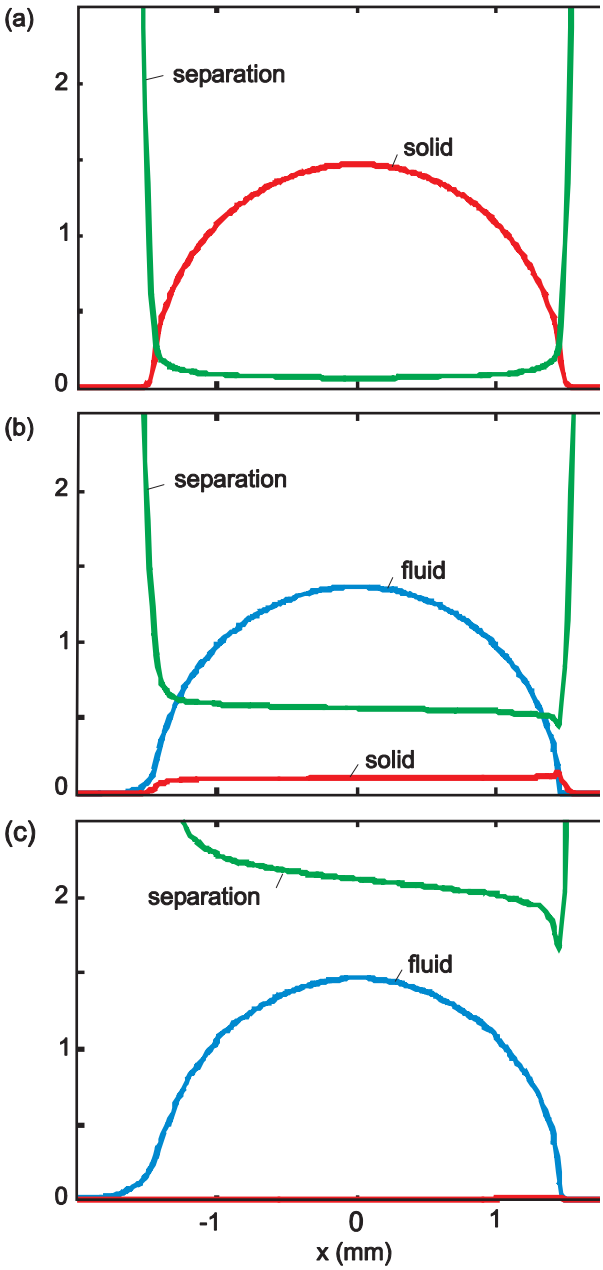

Fig. 12: *Simulation results for three different velocities U: a) U=0 m/s, b) U=0.05 m/s, c) U=0.5 m/s. Pressures are scaled with 0.1 MPa, separation is scaled in µm*

The dynamic simulation is done within the velocity range of up to 3.3 m/s with a resolution of 0.005 m/s. In Fig. 13 the resulting friction force from experiment and from calculation are compared for equal conditions. In the calculation a constant contact friction coefficient $\mu = 0.5$ has been used. This value is very close to the theoretical prediction, shown in Fig. 9, in the relevant (mixed lubrication) velocity range $0.03\ m/s < v < 0.3\ m/s$ for which experimental data exist. In Fig. 13 the same friction coefficient $\mu=0.5$ is used for all velocities since otherwise it would be hard to disentangle the influence of the hydrodynamic effects on the friction. However, the actual friction predicted for $v < 0.03$ m/s can be accurately obtained by just scaling the calculated friction coefficient with the factor $\mu(v)/0.5$ (or on the log-scale in Fig. 13 by adding the factor $\log[\mu(v)/0.5]$) where $\mu(v)$ is given by Fig. 9.

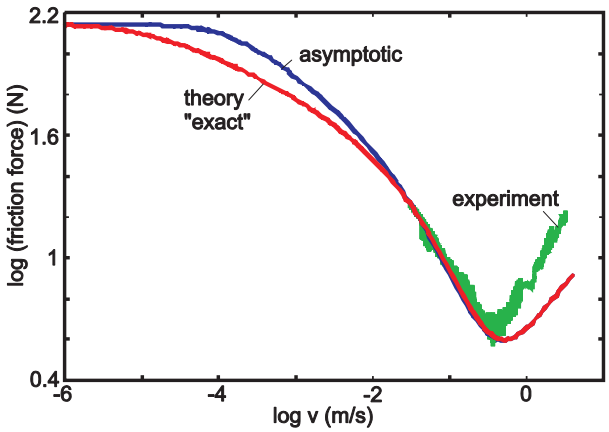

Fig. 13: *Comparison of measurement and simulation*

At the velocity of about 0.4 m/s the solid contact pressure becomes negligible, and a full separation between seal and surface occurs. The theory deviates from experiment in the hydrodynamic region. This is probably due to the insufficient lubrication mentioned before and to the approximation of constant sliding velocity assumed in the numerical model.

6 Conclusion

A simulation model for hydraulic rubber o-ring seals in dynamic application has been presented. Both parts of the model, the FEA based structural analysis to describe the quasi-static behaviour of the seal, as well as the dynamical calculations to describe the boundary-to-hydrodynamic transition, are performed. Characteristic diagrams obtained from the FEA, to be used as auxiliary dimension tool for o-ring seals, were presented. A test rig to measure the friction forces at seals for translational velocities up to 10 m/s was developed. Measurements at this test rig were used to test the simulation model. There is a good agreement between simulation and measurement, especially in the velocity range where mixed lubrication occurs. A deviation at higher velocities is attributable to insufficient lubrication in the experiment and to the approximation of constant sliding velocity in the numerical model.

The design of the test rig will be improved in order to be able to avoid insufficient lubrication conditions. A device to measure the film thickness of the oil film behind the seal will be integrated. Furthermore, the implemented theory of rubber friction will be extended to the one presented by Carbone, Lorenz, Persson and Wohlers (2009) to be able to consider anisotropic surface properties in a more exact way.

Acknowledgments

The authors would like to thank Marcus Liebmann from the institute of physics at RWTH Aachen University for providing the atomic force microscope measurements.

Nomenclature

d	Tube diameter	[m]
E	Young's modulus	[N/m²]
F_{cont}	Boundary friction force	[N]
F_{fluid}	Fluid friction force	[N]
F_{fric}	Friction force	[N]
K	Adjustment factor	[-]
n	Power law exponent	[-]
p	Normal pressure	[Pa]
p_{cont}	Contact pressure	[Pa]
$p_{\text{fluid,dyn}}$	Hydrodynamic fluid pressure	[Pa]
$p_{\text{fluid,stat}}$	Static fluid pressure	[Pa]
t	Time	[s]
u	Average sealing gap	[m]
U	Relative velocity	[m/s]
$\overline{u}$	Elastic seal deformation	[m]
u_0	Un-deformed separation	[m]
x	Axial coordinate	[m]
y	Circumferential coordinate	[m]
z	Radial coordinate	[m]
α	Parameter for asymptotic separation relation	[-]
β	Parameter for asymptotic separation relation	[-]
η	Dynamic viscosity	[Pa s]
α_η	Viscosity-pressure-coefficient	[Pa^{-1}]
β_η	Viscosity-temperature-coefficient	[K^{-1}]
σ	Composite rms roughness	[m]
τ	Shear stress	[N/m²]
E^*	Effective elastic modulus	[N/m²]
h_{rms}	Root-mean-square wave height	[m]
$\mathbf{q}$	Wave vector	[m^{-1}]
P(q)	(Apparent) Normalized area of real contact when looking the contact domain at some given magnification q	[-]
C	Power Spectral Density	[m^4]
ν	Poisson's ratio	[-]
σ_0	Mean perpendicular pressure	[N/m²]

References

Achenbach, M. and **Frank, E.** 2001. Reibung von Elastomeren. *Tribologie und Schmierungstechnik*, Vol. 48, pp. 43-47.

Blok, H. 1963. Inverse Problems in Hydrodynamic Lubrication and Design Directives for Lubricated Flexible Surfaces. *Proceedings of the International Symposium on Lubrication and Wear*, Houston, pp. 9-151.

Bunt, B. P. 1961. Measurement of thickness of thin transparent films using fluorescence. *British Journal of Applied Science*, Vol. 12, pp. 175-177.

Carbone, G., **Lorenz, B.**, **Persson, B. N. J.** and **Wohlers, A.** 2009. Contact mechanics and rubber friction for randomly rough surfaces with anisotropic statistical surfaces. *European Physical Journal E*, Vol. 29, pp. 275-284.

Field, G. J. and **Nau, B. S.** 1975. A theoretical study of the elastohydrodynamic lubrication of reciprocating rubber seals. *Transactions of the American Society of Lubrication Engineers*, Vol. 18, pp. 48-54.

Greenwood, J. A. and **Williamson, J. B. P.** 1966. Contact of Nominally Flat Surfaces. *Proceedings of the Royal Society of London*. Series A, Mathematical and Physical Sciences, Vol. 295, pp. 300-319.

Gropp, A. and **Freitag, E.** 2002. Untersuchung des Dichtmechanismus bei Kolbenstangen-Dichtungen. *12th International Sealing Conference*, Stuttgart, pp. 415-433.

Horcas, I., **Fernández, R.**, **Gómez-Rodríguez, J. M.**, **Colchero, J.**, **Gómez-Herrero, J.** and **Baro, A. M.** 2007. WSXM: A software for scanning probe microscopy and a tool for nanotechnology. *Review of Scientific Instruments*, Vol. 78, 013705.

Johnson, K. L. 2003. *Contact Mechanics.* Cambridge University Press.

Kanters, A. F. C. 1991. On the Elastohydrodynamic Lubrication of Reciprocating Elastomeric Seals: The Influence of the Surface Roughness. *Proceedings of the 17th Leeds-Lyon Symposium on Tribology*, pp. 357-364.

Kanzaki, Y., **Kawahara, Y.** and **Kaneta, M.** 1997. Oil film behaviour and friction characteristic in reciprocating rubber seals: Part 1: Single contact. *Proceedings of the 15th BHR Group International Conference on Fluid Sealing*, London, pp. 79-95.

Nikas, G. K. 2003. Elastohydrodynamics and mechanics of rectangular elastomeric seals for reciprocating piston rods. *Journal of Tribology*, Vol. 125, pp. 60-69.

Nißler, U. and **Haas, W.** 2008. Unterschiede in der Dichtheitsbewertung durch verschiedene Bewertungsverfahren. *Proceedings of the 15th International Sealing Conference*, Stuttgart, pp. 355-368.

Öngün, Y., **Andre, M.**, **Bartel, D.** and **Deters, L.** 2008. An axisymmetric hydrodynamic interface element for finite-element computations of mixed lubrication in rubber seals. *Journal of Engineering Tribology*, Vol. 222, pp. 471-481.

Patir, N. and **Cheng, H. S.** 1978. An Average Flow Model for Determining Effects of Three-Dimensional Roughness on Partial Hydrodynamics Lubrication. *Journal of Lubrication Technology*, Vol. 100, pp. 12-17.

Patir, N. and **Cheng, H. S.** 1979. Application of Average Flow Model to Lubrication Between Rough Sliding Surfaces. *Journal of Lubrication Technology*, Vol. 101, pp. 220-230.

Persson, B. N. J. 2001. Theory of Rubber Friction and Contact Mechanics. *Journal of Chemical Physics*, Vol. 115, pp. 3840-3861.

Persson, B. N. J. and **Scaraggi, M.** 2009. On the transition from boundary lubrication to hydrodynamic lubrication in soft contacts. *Journal of Physics: Condensed Matter*, Vol. 21, 185002.

Persson, B. N. J. 2007. Contact mechanics: relation between interfacial separation and load. *Physical Review Letters*, Vol. 99, 125502.

Raparelli, T., **Bertetto, A. M.** and **Mazza, L.** 1997. Experimental and numerical study of friction in an elastomeric seal for pneumatic cylinders. *Tribology International*, Vol. 30, pp. 547-552.

Reddyhoff, T., **Dwyer-Joyce, R.** and **Harper, B.** 2006. Ultrasonic measurement of film thickness in mechanical seals. *Sealing Technology*, Vol. 2006, pp. 7-11.

Ruskell, L. E. C. 1980. A rapidly converging theoretical solution of the elastohydrodynamic problem for rectangular rubber seals. *Journal of Mechanical Engineering Science*, Vol. 22, pp. 9-16.

Salant, R. F., **Maser, N.** and **Yang, B.** 2007. Numerical Model of a Reciprocating Hydraulic Rod Seal. *Journal of Tribology*, Vol. 129, pp. 91-97.

Wassink, D. B, **Lenss, V. G.**, **Levitt, J. A.** and **Ludema, K.C.** 2001. Physically Based Modeling of Reciprocating Lip Seal Friction. *Journal of Tribology*, Vol. 123, pp. 404-412.

Wernecke, P. W. 1983. *Untersuchung der physikalischen Vorgänge in Spalten von Hydraulikdichtungen.* Doctoral Thesis, RWTH Aachen University.

White, C. M. and **Denny, D. F.** 1947. The sealing mechanism of flexible packings. *Scientific and Technical Memorandum 3/47*, Ministry of Supply.

Williams, M. L., **Landel, R. F.** and **Ferry J. D.** 1955. The Temperature Dependence of Relaxation Mechanisms in Amorphous Polymers and Other Glass-forming Liquids. *Journal of the American Chemical Society*, Vol. 77, pp 3701-3707.

Winney, P. E. 1968. The thickness measurement of thin fluid films by a magnetic reluctance technique. *Journal of Scientific Instruments (Journal of Physics E) Series 2*, Vol. 1, pp. 767-769.

Alexander Wohlers
Born in 1979 in Saarburg, Germany. Studied mechanical engineering at the University of Applied Sciences Trier. Finished his diploma thesis in September 2005 in the field of hydraulic seal technology. Since November 2005 he is member of the scientific staff of Institute for Fluid Power Drives and Controls at RWTH Aachen University.

Oliver Heipl
Born in 1982 in Biberach an der Riß, Germany. Studied mechanical engineering at RWTH Aachen University. Finished his diploma thesis in October 2008 in the field of static and dynamic simulation of reciprocal pneumatic O-Ring-Seals. Since November 2008 he is member of the scientific staff of Institute for Fluid Power Drives and Controls at RWTH Aachen University.

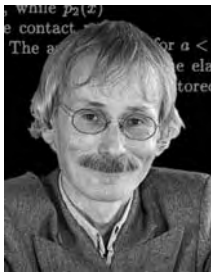

Bo N. J. Persson
Born in 1952, is a research scientist at IFF, Research Center Jülich. Presently his main research activity is in tribology (adhesion, friction and contact mechanics) and surface science, in particular dynamical processes at surfaces, and biophysics.

Michele Scaraggi
Born in 1982 in Terlizzi, Italy. Studied mechanical engineering at the Technical University of Bari, Italy. Finished his diploma thesis in November 2006 in the field of MEMS technology. Since January 2007 he is member of the scientific staff of Department of Mechanical Engineering at the Technical University of Bari.

Hubertus Murrenhoff
Born in 1953 he is Director of the Institute for Fluid Power Drives and Controls (IFAS) at RWTH Aachen University, Germany. Main research interests cover hydraulics and pneumatics including components, systems, controls, simulation programs and the applications of fluid power in mobile and stationary equipment.